

Theory of nonadiabatic transitions in a system of three charged particles

S. Yu. Ovchinnikov and E. A. Solov'ev

A. A. Zhdanov State University, Leningrad

(Submitted 18 August 1985)

Zh. Eksp. Teor. Fiz. **90**, 921-932 (March 1986)

The singular points in the terms in the problem of two Coulomb centers are studied in the complex plane of the internuclear distance R in a continuation of work begun previously by the second author [Zh. Eksp. Teor. Fiz. **81**, 1681 (1981) [Sov. Phys. JETP **54**, 893 (1981)]].

New series of singular points, associated with "hidden" quasicrossings, are found. In general, these series partition the entire positive axis of internuclear distances into four intervals (A , B , C , and D), in each of which the region of the classically allowed motion of an electron has a specific topology. In the adiabatic approximation, inelastic transitions occur only at the boundaries between intervals A , B , C , and D or when an isolated quasicrossing is passed at large R in interval D . The ionization $H + p \rightarrow p + p + e$ is studied as an example.

1. INTRODUCTION

The analytic properties of the terms (the molecular potential curves) $E(R)$ in the complex plane of the internuclear distance R play a major role in the adiabatic approximation. Nonadiabatic transitions between two terms $E_1(R)$ and $E_2(R)$ are associated with a complex branch point R which these terms share and near which the difference $\Delta E(R) = E_1(R) - E_2(R)$ can be described by¹

$$\Delta E(R) = \text{const} (R - R_c)^{1/2}. \quad (1)$$

Branch points occur in pairs R_c, R_c^* (the asterisk means the complex conjugate) in the complex R plane. When a single loop is made around each such point, the terms are interchanged [see (1)]; i.e., the two terms are different sheets of the same analytic function. The probability for a transition between terms E_1 and E_2 which is associated with the branch point R_c is determined by the Massey parameter

$$\Delta = \left| \text{Im} \int_{\text{Re } R_c}^{i(R_c)} \Delta E(R(t)) v dt \right|. \quad (2)$$

Specifically, this probability is¹

$$q = \exp(-2\Delta/v), \quad (3)$$

where v is the initial velocity of the colliding atomic particles. When $\text{Im} R_c$ is small, the branch point is manifested as a quasicrossing of a pair of terms on the real axis.

In calculations on specific processes in the adiabatic approximation, the basic difficulties are in finding the terms, since the spectral problem does not have an asymptotic parameter (in contrast with the dynamic problem, where $v \ll 1$ is such a parameter), and the only mathematically correct way to solve the problem is by numerical calculation. The situation is eased considerably when the transition occur at large internuclear distances. In such cases we can use R as a large parameter and analytically calculate the terms of a quasimolecule in terms of the characteristics of its constituent atoms.² Furthermore, quasicrossings at large distances are generally very narrow and clearly defined, so that condi-

tion $\Delta \ll 1$ holds for them, and the Massey parameter can be expressed, with the help of the Landau-Zener model, in terms of the characteristics of the terms on the real R axis. These quasicrossings play an important role in the physics of a low-temperature plasma, since the smallness of the Massey parameter causes the Landau-Zener transitions to reach a maximum at the low collision velocities, $v \approx \Delta$, which are characteristic of a low-temperature plasma. The combination of a high transition probability with large impact parameters ρ ($\rho \approx \text{Re} R_c \gg 1$) leads to cross sections which are comparable to or greater than the cross section from gas kinetics.

Developments in the physics of fusion plasmas have recently attracted more interest to the velocity region $v \approx 1$ a.u. At such velocities the narrow quasicrossings at large distances are passed in a diabatic manner by the quasimolecule, and the corresponding cross sections are small. Here wide quasicrossings, with a Massey parameter $\Delta \approx 1$ a.u. are more important. These quasicrossings are greatly distorted by nearby terms, to the extent that they become indistinguishable in the overall pattern of terms. In this situation we cannot use a simple model parametrization of Δ in terms of the characteristics of the terms at real values of R even in calculating the Massey parameter (2). In some cases, a direct numerical calculation of the terms in the complex R plane is necessary even to find the quasicrossing itself. The most natural system for a study of such "hidden" quasicrossings is the problem of two Coulomb centers. On the one hand, the variables can be separated in the prolate spheroidal coordinates ξ, η, φ in this problem, and there is a comparatively simple algorithm for calculating the terms in the complex R plane. On the other hand, this system contains the basic features of a diatomic quasimolecule system. The first such calculation was carried out in Ref. 3, where quasicrossings, of a new type, which give rise just to transitions between bound states but also to ionization, were discovered. In previous analyses (see, e.g., Ref. 4) of the terms on the real R axis these quasicrossings were not noticed because of their severe distortion.

The problem of two Coulomb centers not only reveals

the various types of hidden quasicrossings and the mechanism for their appearance but also yields approximate analytic expressions which relate the parameters of a quasicrossing with the characteristics of the quasimolecule and its quantum numbers.³ These approximate expressions play the same role as a parametrization of Δ with the help of the Landau-Zener model for narrow quasicrossings. These expressions can then be used in more complex situations for calculations on inelastic processes.

In the present paper we continue the study begun in Ref. 3 of the branch points of the terms in the problem of two Coulomb centers in the complex plane of the internuclear (intercenter) distance R . To classify the terms $E(R)$ we will use the spherical quantum numbers n, l, m of a combined hydrogenlike atom, whose energy levels are the limits of the terms $E(R)$ as $R \rightarrow 0$. These quantum numbers are related to the numbers of zeros (k, q , and m) of the wave function in terms of the variables ξ, η , and φ by⁴

$$n = k + q + m + 1, \quad l = q + m.$$

For l and m we will also use spectroscopic notation: $l = s, p, d, \dots$ and $m = \sigma, \pi, \delta, \dots$. We will be using the atomic system of units in this paper.

2. BRANCH POINTS OF THE TERMS OF THE $Z_1 e Z_2$ SYSTEM IN THE SYMMETRIC CASE ($Z_1 = Z_2$)

The problem of two Coulomb centers has two nontrivial parameters: the internuclear distance R and the ratio of the charges of the Coulomb centers, Z_1/Z_2 . In the present section of the paper we examine the structure of the branch points in the complex R plane in the symmetric case, i.e., the case $Z_1 = Z_2$. In the section which follows we analyze the evolution of the branch points as the ratio Z_1/Z_2 changes. We have numerically calculated the terms $E_{nlm}(R)$ in the complex R plane on a BESM-6 computer by the program used in Ref. 3. Before we discuss the results, we will briefly review the results found in Ref. 3 so that we can later draw a complete picture of the analytic structure of the terms.

Branch points R_{nlm}^{n+1lm} which relate pairs of terms $E_{nlm}(R), E_{n+1lm}(R)$ in succession for all $n \geq l+1$ were found in Ref. 3. The branch points R_{nlm}^{n+1lm} with different values of n but a fixed set $\{lm\}$ form an infinite series of points which are localized in a small region Ω of the R plane and which converge on a limit point

$$R_{lm} = \lim_{n \rightarrow \infty} R_{nlm}^{n+1lm}.$$

These branch points combine all the terms of this $\{lm\}$ series into a common analytic function $E_{lm}(R)$. Near (but not in) the region Ω , the function $E_{lm}(R)$ is described accurately by³

$$E_{lm}(R) = -\frac{Z^2}{2[(2\pi i)^{-1} \ln(R - R_{lm})]^2}, \quad (4)$$

where $Z = Z_1 + Z_2$. The expression in square brackets in (4) serves as the principal quantum number in the hydrogen-like spectrum. Near Ω , the energy surface $E_{lm}(R)$ has the shape of a corkscrew, and when a single loop is made around the logarithmic branch point R_{lm} in (4) there is a

transition from the given term $E_{nlm}(R)$ to the neighboring term $E_{n \pm 1lm}(R)$ (\pm depending on the direction in which the loop is made). We denote the series of points $\{lm\}$ as S_{l+1lm} . Since all the points of a given series lie close together in the R plane, we assign the series S_{l+1lm} a definite position, specified by the limiting point R_{lm} . The following approximate expression was derived in Ref. 3 for the series with $m = 0$:

$$R_s \equiv \text{Re } R_{l\sigma} = l(l+1)/Z, \quad \text{Im } R_{l\sigma} = 2l/Z. \quad (5)$$

This expression gives the position of the series $S_{l+1l\sigma}$ within $\sim 10\%$.

In addition to the series $S_{l+1l\sigma}$ studied in Ref. 3, there are other series of branch points in the R plane. We turn now to a description of these other branch points, beginning with the analytic structure of the terms in the H_2^+ system. In this case, since the charges of the nuclei are equal, we have an additional symmetry—the parity—and all the states can be classified as either even (g -states) or odd (u -states).¹ Terms with different values of m or with different parities evidently do not have common branch points, since the symmetry of a state cannot be changed by a continuous change in R . Figure

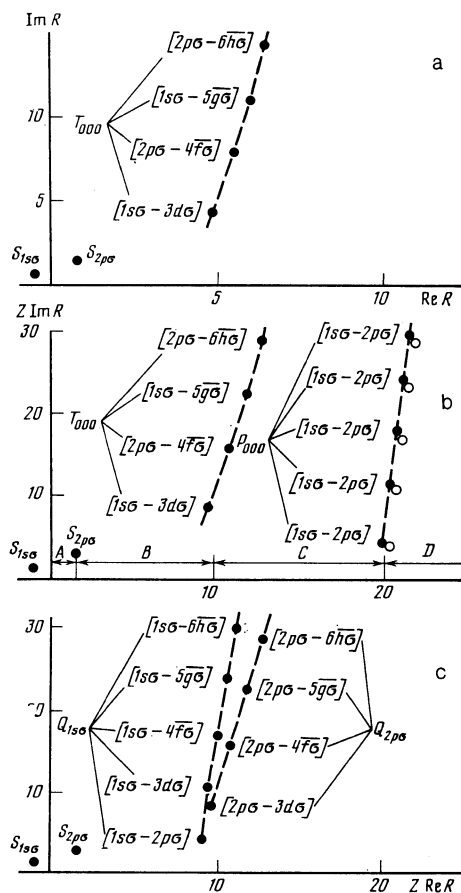


FIG. 1. Branch points of the $1s\sigma$ and $2p\sigma$ terms in the complex R plane for three values of the charge Z_2 ($Z_1 = 1$). a— $Z_2 = 1$; b—1.001; c—1.008. The quantum numbers of the terms related by the given branch point are given in square brackets. The open circles in part b show the positions of the branch points for the difference in terms in (9), with $w(R)$ and δ from (11) and (12). The regions A, B, C, and D for the $2p\sigma$ term are shown.

1a shows the branch points of the $1s\sigma_g$ and $2p\sigma_u$ terms for the molecular ion H_2^+ . In addition to the series $S_{1s\sigma}$ and $S_{2p\sigma}$ we see that there is a series of branch points at $\text{Re}R \approx 5$ a.u. The branch points of the terms $1s\sigma_g$ and $2p\sigma_u$ are combined into a single series because of their behavior in the limit $R \rightarrow \infty$. In the limit $R \rightarrow \infty$, the adiabatic states of the symmetric system H_2^+ become either the sum (g -states) or the difference (u -states) of the two hydrogenlike states which are localized at different nuclei and which have an identical set of parabolic quantum numbers $\{n_1, n_2, m\}$. The quantum numbers of the combined atom which were introduced above are related to these parabolic quantum numbers by⁴

$$l_g = 2n_2 - [(-1)^m - 1]/2, \\ n_g = l_g + n_1 + m + 1$$

for the g -states or

$$l_u = 2n_2 + [(-1)^m + 1]/2, \\ n_u = l_u + n_1 + m + 1$$

for the u -states. A pair of g - and u -terms with an identical set of parabolic quantum numbers is exponentially degenerate at large R . The numerical calculations reveal that each such pair of terms has a common series of branch points with high-lying terms, which we denote as $T_{n_1, n_2, m}$. In these series, we find the following approximate behavior (Fig. 1a): All the branch points in a given series are distributed uniformly on a straight line which runs nearly perpendicular to the real R axis. The spacing between the branch points is

$$\Delta R \approx n_\infty \pi i$$

($n_\infty = n_1 + n_2 + m + 1$ is the principal quantum number of the limiting state as $R \rightarrow \infty$). The branch points on the even term ($n_g l_g m$) and the odd term ($n_u l_u m$) alternate; the j th branch point on the term $n_g l_g m$ relates this term to a g -term:

$$n = n_g + 2j, \quad l = l_g + 2j.$$

The j th point on the term $n_u l_u m$ relates it to a u -term:

$$n = n_u + 2j, \quad l = l_u + 2j$$

($j = 1, 2, 3, \dots$ is the order of the branch point, counted from the real R axis).

The series $T_{n_1, n_2, m}$ arises because a pair of (g, u) terms reaches the top of a barrier separating effective potential wells of two Coulomb centers in the angular equation⁴

$$\frac{d^2\psi}{d\eta^2} + \left[-p^2 + \frac{\lambda}{1-\eta^2} + \frac{1-m^2}{(1-\eta^2)^2} \right] \psi = 0, \quad (6)$$

TABLE I. Exact values of the real part of that branch point $R^{(1)}_{n_1, n_2, m}$ of the series $T_{n_1, n_2, m}$ which is closest to the real R axis; positions of the point R_T at which the term reaches the top of the barrier, calculated from (8) for the H_2^+ system.

$\{n_1, n_2, m\}$	(0, 0, 0)	(1, 0, 0)	(2, 0, 0)	(0, 0, 1)	(0, 1, 0)
$\text{Re}R^{(1)}_{n_1, n_2, m}$	4.75	7.9	10.96	13.4	20.12
R_T	4.0	8.0	12.0	13.6	20.9

where $p = (-2E)^{1/2}R/2$, and λ is a separation constant. We can estimate the value R_T at which the energy level touches the top of the barrier from the asymptotic expressions for p and λ in the limit $R \rightarrow \infty$ (Ref. 4):

$$p = R/2n_\infty, \quad \lambda = 2p(2n_2 + m + 1) - [(2n_2 + m + 1)^2 + 1 - m^2]/2. \quad (7)$$

In this approximation the two terms of the (g, u) pair are coincident, and they reach the barrier simultaneously. Substituting (7) into the effective potential for Eq. (6), and using the condition that the energy level touches the top of the barrier, we find

$$R_T = 2n_\infty [2n_2 + m + 1 + [(2n_2 + m + 1)^2 + 1 - m^2]/2]^{1/2}. \quad (8)$$

Table I compares values calculated from (8) with the real part of the branch point nearest the real axis for several series $T_{n_1, n_2, m}$. We see from this table that expression (8) gives a correct description of the behavior of the position of the series as a function of the quantum numbers.

3. BRANCH POINTS OF THE TERMS OF A $Z_1 e Z_2$ SYSTEM WITH $Z_1 \neq Z_2$

In the case $Z_1 \neq Z_2$ we lose the exact (g, u) symmetry, and additional series of branch points arise. Figure 1b shows branch points of the $1s\sigma$ and $2p\sigma$ potential curves for $Z_1 = 1$ and $Z_2 = 1.001$. In addition to the series $S_{1s\sigma}$, $S_{2p\sigma}$, and T_{000} we see a new series of branch points, P_{000} . These points have approximately the same real part, $R_p \approx 10$ a.u. In the limit $Z_2 \rightarrow Z_1$, this series goes off to infinity along the positive real R semiaxis. The series $P_{n_1, n_2, m}$ arises by virtue of the Rosen-Zener-Demkov interaction.⁵

The two-level Rosen-Zener-Demkov model is ordinarily used in calculations on charge exchange with a small resonance defect. In this model, the splitting of terms is described by

$$\Delta E(R) = [\delta^2 + w^2(R)]^{1/2}, \quad (9)$$

where δ is the splitting of terms in the limit $R \rightarrow \infty$ (the resonance defect), and the function $w(R) = \alpha \exp(-\beta R)$ models the exchange interaction of diabatic states. The regions in which the transitions are nonadiabatic is the region with $\delta \approx |w(R)|$. Here the splitting in (9) has an infinite, equidistant sequence of branch points

$$R_{j, \pm} \approx R_p \pm i\pi(j + 1/2)/\beta, \quad j = 0, 1, 2, \dots, \quad (10)$$

where $R_p = (1n\alpha/\delta)/\beta$. The two energy surfaces are uniformly joined by these branch points along a line running perpendicular to the real R axis. Expression (10) gives a

qualitative description of the structure of the branch points $P_{n_1, n_2, m}$. More accurate values can be found for the branch points if we use for the exchange interaction $w(r)$ its asymptotic expression in the limit $R \rightarrow \infty$ in the problem of two Coulomb centers with $Z_1 = Z_2 = 1$ (Ref. 4):

$$w_c(R) = 2(2R/n_\infty)^{n_\infty - n_1 + n_2} \times \exp(-n_\infty - R/n_\infty) / [n_\infty^3 n_2! (n_2 + m)!]. \quad (11)$$

The resonance defect in our case is

$$\delta = (Z_2^2 - Z_1^2) / 2n_\infty^2. \quad (12)$$

Using $w_c(R)$ and δ from (11) and (12) in (9), we can numerically solve the transcendental equation $\delta = \pm iw_c(R)$ to find the positions of the branch points; in the case $Z_2 = 1.001$ the results are essentially identical to the exact values (Fig. 1b). There are series $P_{n_1, n_2, m}$ for all pairs of states which are localized at different centers in the limit $R \rightarrow \infty$ and which have an identical set of parabolic quantum numbers $\{n_1, n_2, m\}$. These series are related to a breaking of the approximate (g, u) symmetry. To the left of the $P_{n_1, n_2, m}$ series we can ignore the resonance defect in comparison with the exchange interaction, and the situation is qualitatively close to the symmetric case $Z_1 = Z_2$. To the right of this series, the resonance defect dominates, and the approximate (g, u) symmetry is lost.

As the charge Z_2 is increased further, the positions of the branch points on the $1s\sigma$ and $2p\sigma$ sheets change in the following way. The series $S_{1s\sigma}$, $S_{2p\sigma}$, and T_{000} initially remain essentially in place, while the series P_{000} moves as a whole to the left. At $Z_2 \approx 1.07$, the points of the P_{000} series pass between the branch points of the T_{000} series. The structure of the Riemann surface undergoes a qualitative change, and the series P_{000} undergoes a continuous conversion into the series $Q_{1s\sigma}$, and the series T_{000} does the same, into the series $Q_{2p\sigma}$. In each of the series Q_{nlm} the branch points relate the initial term ($1s\sigma$ or $2p\sigma$) in succession with all terms having the same radial quantum number k (Fig. 1c). The reason for this change in structure is that at $Z_2 \approx 1.07$ we lose the approximate (g, u) symmetry on the large- R side, down to $R = R_T$, and a quasicrossing of terms having different parities at $Z_1 = Z_2$ is no longer approximately forbidden. With a further increase in Z_2 , the $1s\sigma$ and $2p\sigma$ terms reach a barrier at different values of R , so that the terms $Q_{1s\sigma}$ and $Q_{2p\sigma}$, associated with the attainment of this barrier, diverge.

At $Z_2 \approx 1.07$, the series of branch points $P_{n_1, n_2, m}$, characteristic of the Rosen-Zener-Demkov model, thus disappears, and this model no longer applies. Interestingly, the Rosen-Zener-Demkov interaction drops out of the picture at a very small value of the quantum defect δ , only 7% of the distance to the neighboring multiplet.

After the series $Q_{1s\sigma}$ and $Q_{2p\sigma}$, forms on the $1s\sigma$ energy surface, no other important changes occur. In order to describe the subsequent evolution of the singular points on the $2p\sigma$ energy surface we need to simultaneously examine the $3d\sigma$ energy surface.

Figure 2a shows branch points of the $2p\sigma$ and $3d\sigma$ terms for the charges $Z_1 = 1$ and $Z_2 = 1.2$. There are four series

here: $S_{2p\sigma}$, $S_{3d\sigma}$, $Q_{2p\sigma}$, and $Q_{3d\sigma}$. The series $Q_{3d\sigma}$ forms as a result of a change in the structure of the series T_{100} and P_{100} at $Z_2 \approx 1.07$, as discussed above in the case of the formation of the $Q_{1s\sigma}$ and $Q_{2p\sigma}$ series. As Z_2 is increased, the series $Q_{2p\sigma}$ and $Q_{3d\sigma}$ move toward each other, and they merge at $Z_2 \approx 2$, where there is a random degeneracy of the $2p\sigma$ and $3d\sigma$ terms in the limit $R \rightarrow \infty$. At $Z_2 \approx 2.1$, the sheets and branch points are renumbered in such a way that the relationship between the $2p\sigma$ and $3d\sigma$ terms disappears in the series $Q_{2p\sigma}$ (Fig. 2b). At the same time, an isolated branch point $I_{2p\sigma}^{3d\sigma}$, which relates the terms $2p\sigma$ and $3d\sigma$, arises at $R = +\infty$. This branch point then approaches, at $Z_2 \approx 3.5$, the incomplete series $\tilde{Q}_{2p\sigma}$ and complements it to form a standard series (Fig. 2c). The branch point $I_{2p\sigma}^{3d\sigma}$ is related to a quasicrossing of terms which correspond to states localized at the different nuclei. Quasicrossings of this type are quite familiar;^{2,4} they constitute the only case which has previously been discussed in the literature, except in Ref. 3.

For $Z_2 > 3$ the structure of the branch points on the $2p\sigma$ energy surface does not change qualitatively. The series $Q_{3d\sigma}$ makes contact with the $Q_{2p\sigma}$ series and then goes off toward large R where it collides with the series $Q_{4f\sigma}$ at $Z_2 \approx 3.7$. Here there is another renumbering of the sheets as in the collision of the $Q_{2p\sigma}$ and $Q_{3d\sigma}$ series, and an isolated

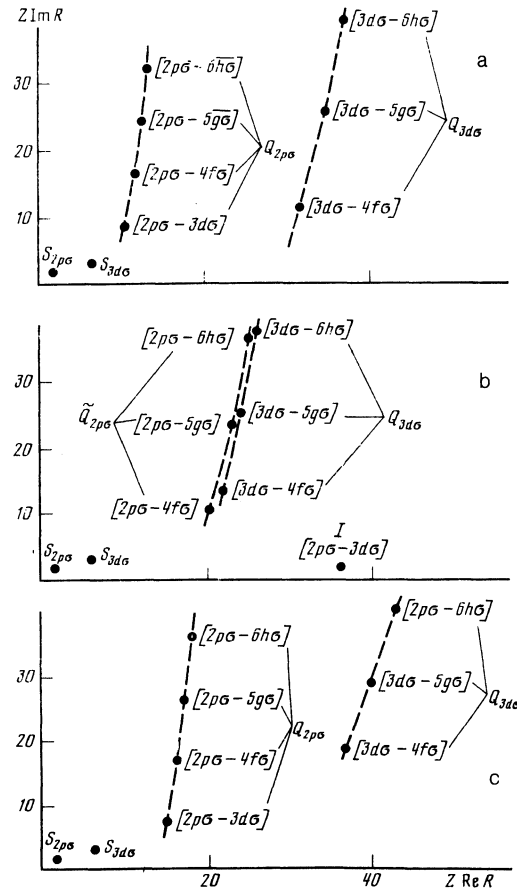


FIG. 2. Branch points of the $2p\sigma$ and $3d\sigma$ terms in the complex R plane for three values of the charge Z_2 ($Z_1 = 1$). a— $Z_2 = 1.2$; b— 2.1 ; c— 3.5 . $Q_{2p\sigma}$ in Fig. 3b means an incomplete $Q_{2p\sigma}$ series.

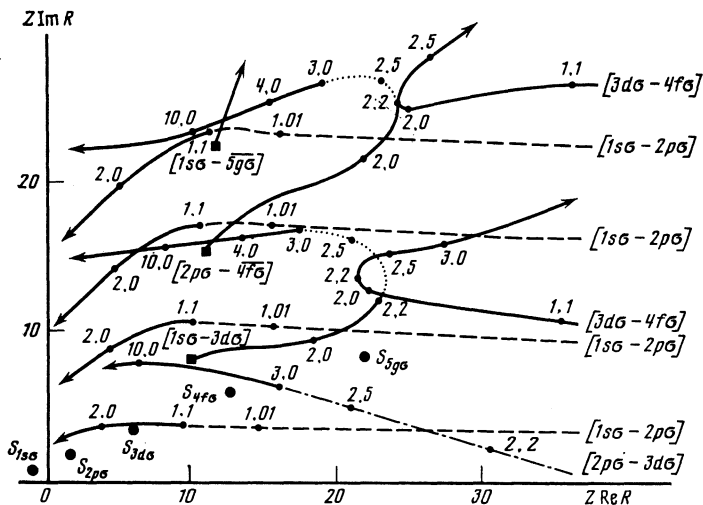


FIG. 3. Trajectories traced out by the branch points of the $1s\sigma$, $2p\sigma$, and $3d\sigma$ terms as the charge Z_2 is changed continuously ($Z_1 = 1$). The numbers labeling the trajectories are the charge Z_2 . Dot-dashed line—trajectory of the isolated branch point $I_{2p\sigma}^{3d\sigma}$; dashed line—trajectory of the $P_{n_1, n_2, m}$ series; solid line—trajectory of the Q_{nlm} series; dotted line—trajectory of the incomplete series \tilde{Q}_{nlm} . In the scale of this figure, the S_{nlm} and $T_{n_1, n_2, m}$ series remain essentially fixed, at the positions shown by the circles and squares, respectively.

branch point $I_{3p\sigma}^{4f\sigma}$, arises at infinity and then attaches to the incomplete series $\tilde{Q}_{3d\sigma}$. This evolution of the series of singular points and isolated branch points $I_{nlm}^{n'l'm}$ is repeated in succession on all the high-lying terms.

Figure 3 shows trajectories of the branch points in the R plane traced out as the charge Z_2 is gradually increased ($Z_1 = 1$). This figure illustrates the overall evolution of the branch points of the $1s\sigma$ and $2p\sigma$ terms; this evolution is also characteristic of all the other terms of the system.

We have one final comment to add to these results of the numerical calculations. When any branch point $R_{nlm}^{n'l'm}$ lies to the left of, and further from the real axis than, the series $S_{l'+1l'm}$ in the R plane (the series $S_{l'+1l'm}$ always lies to the left of such a branch point), then by starting at the term $E_{nlm}(R)$ on the real R axis, looping the branch point $R_{nlm}^{n'l'm}$, and then returning to the real R axis, we end up not at the term $E_{n'l'm}(R)$ but at some virtual or quasisteady term, indicated by $(\bar{n}l'm)$ in the figures. These terms will be discussed in detail in a separate paper.

4. DISCUSSION

These results suggest a reinterpretation of the change in the structure of adiabatic states as the internuclear distance is changed. As $Z_2 \approx Z_1$, the series of singular points S , T , and P partition of the entire positive real R axis into the four intervals A , B , C , and D (Fig. 1b). In each of these intervals, the region of classically allowed motion of an electron has a specific topology, as illustrated in Fig. 4. In interval A ($0 < R < R_S$) both of the nuclei are screened by the centrifugal core of the combined atom, as was shown in Ref. 3, and the electron perceives these nuclei as constituting a single Coulomb center (Fig. 4a). In this interval, it is physically justifiable to replace the exact adiabatic wave function by the simpler wave function of the combined atom. Interval B ($R_S < R < R_T$) has a substantially quasimolecular nature (Fig. 4b). In this interval, even in the crudest approximation, we need to take into account the difference between the positions of the nuclei (in contrast with the case in interval A), and we need to consider the interaction of the electron

with the two nuclei simultaneously (in contrast with interval C). In interval C ($R_T < R < R_P$) the regions of classically allowed motion near the two nuclei are separated by a barrier (Fig. 4c), and here the wave function can be approximated as a superposition (symmetric or antisymmetric) of the wave functions of two isolated atoms Z_1e and Z_2e . In interval D ($R_P < R < \infty$), we do not have the approximate (g, u) symmetry, and the wave function is approximately the wave function of an isolated atom, either Z_1e or Z_2e (Fig. 4d). When we go from one interval to another, we see a qualitative change in the structure of the adiabatic state, as reflected in the series of singular points.

This partitioning into four intervals A , B , C , and D does not always occur. For s -terms, series S lies in the left-hand R half-plane, so that there is no interval A in these cases. Furthermore, when, with increasing Z_2 , series T and P merge (Fig. 1c), the interval of approximate (g, u) symmetry, C is lost. In the symmetric case ($Z_1 = Z_2$) there is no interval D .

One might get the impression that although the results found here do paint an elegant picture of how all the terms of

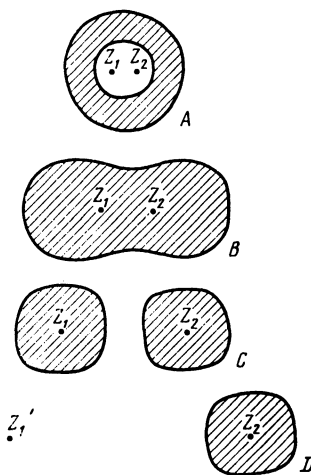


FIG. 4. Schematic drawing of the regions of classically allowed motion of an electron (the hatched region) in the intervals A , B , C , and D .

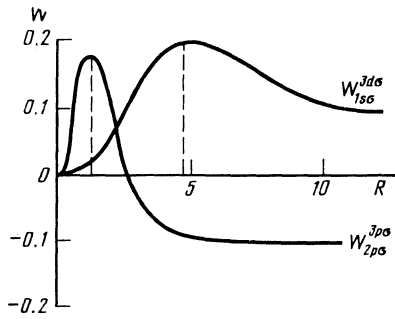


FIG. 5. Matrix elements of the nonadiabatic coupling of $W_{1s\sigma}^{3d\sigma}$ and $W_{2p\sigma}^{3p\sigma}$ for the H_2^+ system.

a given symmetry combine into a common analytic function of R , the behavior of the terms at real values of R is not noticeably affected by the presence of branch points, so that these points play no role in the theory of nonadiabatic transitions. This impression would be wrong. According to the general theory,¹ a transition probability (3) is associated with any branch point, and this probability will of course decrease with increasing distance from the branch point to the real R axis. The region in which the adiabatic states interact strongly may not be strikingly obvious in the pattern of terms at real R (the terms of the Rosen-Zener-Demkov model might serve as an example here). More sensitive are the matrix elements of the nonadiabatic coupling between states which are coupled by the given branch point $R_{nlm}^{n'l'm}$:

$$W_{nlm}^{n'l'm} = \left\langle nlm \left| \frac{d}{dR} \right| n'l'm \right\rangle.$$

Figure 5 shows the nonadiabatic-coupling matrix elements taken from Ref. 6. We see that the matrix elements $W_{nlm}^{n'l'm}$ between states having a common branch point $R_{nlm}^{n'l'm}$ have a clearly defined maximum on the real R axis near this branch point. This result is not surprising since at the branch points R_c the corresponding matrix elements become infinite and have a first-order pole: $W \approx (R - R_c)^{-1}$. The bell shape of the matrix elements on the real axis is a reflection of these poles in the complex plane; i.e., the presence of a branch point for the terms and the presence of a maximum for the matrix elements are interrelated phenomena. It is because of this fact that we can calculate the probabilities for inelastic transitions in the adiabatic approximation knowing nothing more than the terms [see (2) and (3)]—there is no need to calculate the nonadiabatic-coupling matrix elements.

It follows that in the adiabatic approximation transitions between terms occur at the boundaries of intervals A , B , C , and D and also when an isolated branch point I in interval D is passed. Knowing the positions of the branch points and the splitting of the terms on the real R axis, we can easily estimate the Massey parameters in (2) for these hidden quasicrossings. As an example we consider the ionization



As the nuclei on each other, the ground state of the hydrogen

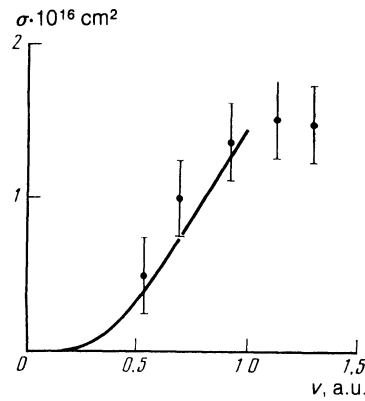


FIG. 6. Cross section for the ionization $H + p \rightarrow p + p + e$. Solid line—ionization cross section calculated from (15); circles—experimental data.⁸

becomes a superposition of $1s\sigma$ and $2p\sigma$ states of the quasi-molecule. The ionization in this case occurs from the $2p\sigma$ term as a result of nonadiabatic transitions through an infinite chain of hidden quasicrossings associated with the series $S_{2p\sigma}$. In the approximation of a rectilinear passage ($R^2 = \rho^2 + v^2 t^2$) the total Massey parameter for this process is³

$$\Delta = \Delta_0 (1 + \rho^2 / 2 |R_{p\sigma}|^2), \quad (14)$$

where $|R_{p\sigma}|^2 \approx 1.5$, and $\Delta_0 \approx 0.4$ is the Massey parameter at $\rho = 0$. Substituting (14) into (3), and integrating over the impact parameters, we find the ionization cross section:

$$\sigma = 2\pi \int_0^\infty \rho d\rho \exp^{-2\Delta/v} = 3.75\pi v \exp^{-0.8/v}. \quad (15)$$

Two other factors, which tend to cancel each other out, are incorporated in (15). First, there is the circumstance that the initial population of the $2p\sigma$ term is $1/2$; there is the circumstance that the region of nonadiabatic transitions is crossed twice, as the nuclei close on each other and as they move apart. Figure 6 shows the experimental ionization cross section⁸ and that calculated from expression (15). We see that despite the approximate nature of (15) there is a good agreement with experiment in the range of applicability of the adiabatic approximation. Convincing evidence of the existence of this ionization mechanism was recently found in Ref. 9 in an analysis of experimental data on the spectra of emitted electrons.

The quasicrossings which we have been discussing here are broad, and the associated transitions become noticeable even at rather high collision velocities v . We are thus led to inquire about the applicability of the adiabatic approximation at these velocities. From the mathematical standpoint the adiabatic approximation is an asymptotic expansion of the solution of a dynamic problem (a time-varying Schrödinger equation) in the small parameter v . In general, there is no rigorous quantitative measure of the applicability of such an approximation. A physically plausible assumption is that for each specific transition this approach is applicable up to the maximum of the cross section, i.e., at $v \leq \Delta$.

The results of this study have applications going beyond

calculations on various inelastic processes in the adiabatic approximation. They can also be used to select systematically the most important adiabatic states in the strong-coupling method for specific reaction channels.

In a study of $2p\sigma$ - $np\sigma$ transitions, Henri *et al.*¹⁰ questioned the reality of transitions driven by hidden quasicrossings associated with the series $S_{2p\sigma}$, which had been discussed in Ref. 3. However, it is not clear from the text of their paper just which assertions in Ref. 3 Henri *et al.* believe are wrong or why. The results derived in Ref. 3 were based on an exact calculation of the terms of the problem of two Coulomb centers. Those results follow from a general, mathematically rigorous theory of inelastic transitions in the adiabatic approximation,^{1,2,7} with which Henri *et al.*¹⁰ appear to be unacquainted. An attempt was made in the second section in Ref. 10 to construct diabatic terms, which were introduced in a qualitative way in Ref. 3 to illustrate possible inelastic transitions through hidden quasicrossings associated with the series $S_{2p\sigma}$. For this purpose, the matrix of the total Hamiltonian in the atomic basis was broken up into two blocks and then diagonalized in each block. This procedure is a formal procedure in this case and does not reflect the essence of the matter, so that we are not at all surprised to find that the behavior of the resulting diagonal matrix elements does not agree with the diabatic correlation diagram in Ref. 3. The introduction of diabatic states in this case is a complex problem (as was pointed out in Ref. 3) and requires a more systematic approach. In the third section of Ref. 10, Henri *et al.* derived scaling laws for the nonadiabatic-coupling matrix elements, but those laws do not—despite the assertion of the authors—by themselves explain why the matrix elements are bell-shaped at $R \approx 1$ a.u. As we mentioned earlier (see also Ref. 3), this shape can be explained in a simple way on the basis of the series of branch points $S_{2p\sigma}$. The results calculated on the probability for $2p\sigma$ - $np\sigma$ transitions by the strong-coupling method which Henri *et al.* presented in the fourth section of their paper are not convincing, since they did not solve the problem of dealing with the

translational factor. Instead, the integration of the strong-coupling equations was artificially terminated at $R = 2$ a.u., where the matrix elements $W_{2p\sigma}^{np\sigma}$ depend most strongly on R (Fig. 5). The problem of the translational factor is a general one for the strong-coupling method. It arises because the adiabatic basis is not matched with the physical boundary conditions in the limit $R \rightarrow \infty$. As a consequence, there is a constant component at large R in the nonadiabatic-coupling matrix elements, and this constant component leads to transitions which do not decay as $R \rightarrow \infty$. One possibility for solving this problem was proposed in Refs. 11.

We wish to thank Yu. S. Gordeev, Yu. N. Demkov, I. V. Komarov, E. E. Nikitin, V. I. Osherov, and L. I. Ponomarev for useful discussions.

¹L. D. Landau and E. M. Lifshitz, *Kvantovaya mekhanika*, Nauka, Moscow, 1974 (Quantum Mechanics: Non-Relativistic Theory, Pergamon, New York, 1977).

²E. E. Nikitin and B. M. Smirnov, *Usp. Fiz. Nauk* **124**, 201 (1978) [*Sov. Phys. Usp.* **21**, 95 (1978)].

³E. A. Solov'ev, *Zh. Eksp. Teor. Fiz.* **81**, 1681 (1981) [*Sov. Phys. JETP* **54**, 893 (1981)].

⁴I. V. Komarov, L. I. Ponomarev, and S. Yu. Slavyanov, *Sferoidal'nye i kulonovskie sferoidal'nye funktsii* (Spheroidal and Coulomb Spheroidal Functions), Nauka, Moscow (1976).

⁵Yu. N. Demkov, *Zh. Eksp. Teor. Fiz.* **45**, 195 (1963) [*Sov. Phys. JETP* **18**, 138 (1964)].

⁶L. I. Ponomarev, T. P. Puzynina, and N. F. Truskova, *J. Phys. B* **11**, 3861 (1978).

⁷E. A. Solov'ev, *Vestn. LGU* No. 4, 10 (1976).

⁸W. L. Fite, R. F. Stebbings, D. G. Hummer, and R. T. Brackman, *Phys. Rev.* **119**, 663 (1960).

⁹Yu. S. Gordeev, A. N. Zinoviev, and S. Yu. Ovchinnikov, *Abstracts of XII ICPEAC*, Gatlinburg, 1981.

¹⁰G. Henri, V. Sidis, and C. Kubach, *J. Phys. B* **18**, 691 (1985).

¹¹E. A. Solov'ev, *Teor. Mat. Fiz.* **28**, 240 (1976); E. A. Solov'ev and S. I. Vinitsky, *J. Phys. B.* **18**, L557 (1985).

Translated by Dave Parsons